V European Conference on Computational Fluid Dynamics
ECCOMAS CFD 2010
J. C. F. Pereira and A. Sequeira (Eds)
Lisbon, Portugal,14-17 June 2010

PARAMETRIC UNCERTAINTY QUANTIFICATION IN MODELING METHANE THERMAL PARTIAL OXIDATION WITHIN INERT POROUS MEDIA

Miguel A.A. Mendes, José Manuel C. Pereira and José Carlos F. Pereira

Mechanical Eng. Department - Instituto Superior Técnico,
Pav. Mec. I, 1 andar (LASEF), Av. Rovisco Pais n1,1049-001, Lisbon, Portugal
e-mail: {miguel.mendes,jose.chaves,jcfpereira}@ist.utl.pt

Key words: uncertainty quantification, polynomial chaos, non-intrusive, porous media, thermal partial oxidation

Abstract. *Propagation of parametric uncertainty through a physical model is investigated for the problem of methane thermal partial oxidation within inert porous media. This reforming process is typically used to produce synthesis-gas (rich in H2 and CO) that is important for the hydrocarbon synthesis industry, as well as for some fuel cell type operation. The premixed combustion model includes detailed chemistry and solves the gas- and solid-phase energy balances coupled by convective heat exchange, including radiative heat transfer in the solid-phase. The uncertainty quantification problem is addressed using a non-intrusive spectral projection based method, which allows one to use the original deterministic model without requiring modifications in the source code. The present study focusses on uncertainties existing in the parameters related with the porous media heat transfer phenomena. The uncertain parameters are considered to have a half circle Beta distribution and their probabilistic information is estimated based on producers or experimental sources. Numerical predictions of the model stochastic solutions are obtained for temperature and species profiles and for the laminar burning velocity. The numerical results denote that the uncertainties in the model parameters are relevant for confidence on predicting the synthesis-gas constitution and the burning velocity.*

1 INTRODUCTION

High Temperature Fuel Cell based systems, operating on the basis of synthesis-gas (consisting mainly of H_2 and CO) generated from hydrocarbon reforming, are an efficient way of using hydrocarbon fuels. Among all the conventional hydrocarbon fuels, methane is widely available in nature and has the higher hydrogen to carbon volumetric ratio; therefore, it is potentially suitable for synthesis-gas production.

Among the several techniques used to produce synthesis-gas from hydrocarbons, the Thermal Partial Oxidation (TPOx) offers several advantages, such as: absence of catalysts which eliminates the catalyst deactivation problems; no need for external heat sources and additional feeds like water; good process dynamic response; and applicability to almost all hydrocarbons. However, it shows comparatively low hydrogen yield and the tendency to produce soot [1].

The slow reaction rates at low adiabatic flame temperatures existing in the TPOx process may originate flame instability problems. Therefore, a practical solution is to use Inert Porous Media (IPM) based reactors, in which the higher heat recirculation from the hot products to the reactants, provided by the solid matrix, increases the reaction rates and the stability of the process, improving its operational characteristics when compared to free-flame techniques [2]. Reviews on IPM combustion can be found in [3, 4].

In order to capture the main features of premixed combustion processes within IPM, one-dimensional models are typically employed and, generally, the solid-phase energy balance is solved taking into account radiative heat transfer and is coupled by convective heat exchange with the gas-phase energy balance, see, *e.g.* [5, 6, 7]. A major source of parametric uncertainty in these models is typically related with the conductive, convective and radiative heat transfer phenomenas induced by the IPM, which characterization rely on correlations and coefficients with large uncertainty levels [8, 9, 10]. The value of these parameters depends mainly on the inherent uncertainties existing in the porous material composition and fabrication process [11]. Furthermore, it is important to quantify the accuracy of the numerical predictions in order to establish the confidence intervals for the process behavior, such as, temperatures distribution or exhaust gas composition.

Several stochastic approaches are available nowadays in order to quantify the propagation of uncertainty from the input parameters into the model outputs. Spectral Projection (SP) methods, based on Polynomial Chaos (PC) expansion [12, 13, 14], are more appropriate and suitable for large degree of parametric uncertainty than the computationally expensive Monte Carlo (MC) methods or other methods limited to small uncertainty levels, see, *e.g.* [15, 16]. However, PC based methods require the model parameters to be characterized as aleatory uncertainties, *i.e.*, it is presumed that sufficient probabilistic information exists about the parameters [14]. In SP methods, the uncertain model parameters are made dependent on additional random dimensions along with time and space and the stochastic variables of the model are projected on these random dimensions using appropriate PC expansions. The objective of SP methods is to calculate the PC ex-

pansion mode coefficients, which are then used to extract probabilistic information about the stochastic model solution, such as, statistics, Confidence Intervals (CIs), Probability Density Functions (PDFs) or sensitivity to parametric uncertainty.

SP methods may be formulated using two different approaches: intrusive and non-intrusive [13, 14]. In the Intrusive SP (ISP) approach, the model governing equations are reformulated in order to directly propagate the uncertainty through the model during the simulation, see, *e.g.* [17]. Although this approach is effective, it may not be practically suitable for commercial or complex codes. The Non-Intrusive SP (NISP) approach evaluates *a posteriori* the PC expansion mode coefficients of the stochastic model solution by using deterministic solution samples. This approach shares with MC methods the advantage of using the original deterministic code as a black box. However, as the number of uncertain parameters increases, it requires sophisticated sampling methods to be implemented such that it becomes competitive with the ISP approach [13, 18].

In the present study, the propagation of parametric uncertainty is quantified for a model of methane-air TPOx within IPM by applying the NISP approach. Uncertainty is prescribed in several input parameters related with the IPM heat transfer phenomena. Deterministic solution samples, required for the NISP approach, are obtained with a one-dimensional model that includes detailed chemistry and takes into account the gas- and solid-phase energy balances coupled by convective heat exchange, including radiative heat transfer in the solid-phase. Stochastic solutions are calculated for some relevant variables, such as, temperature and species profiles, and burning velocity, in order to obtain error bars for these solutions and to identify dominant parametric uncertainties.

2 COMPUTATIONAL MODELING

The propagation of parametric uncertainty through the physical model into the output variables is quantified in a non-intrusive manner by using a deterministic model of the methane TPOx process within IPM. This section describes the deterministic model, along with the prescribed uncertain parameters, as well as the algorithm used to quantify the propagation of parametric uncertainty.

2.1 Methane TPOx Model

The methane TPOx process within IPM is simulated with a premixed combustion model that is a modified version of the PREMIX code [19]. The model incorporates the solid-phase energy balance (including radiative heat transfer) and the heat exchange between gas- and solid-phase. The following assumptions are also considered: one-dimensional geometry, laminar combustion, inert homogeneous porous material, constant pressure and negligible catalytic effects. Thus, the governing equations for mass and gas-phase species balance are given as:

Mass Balance

$$\frac{\partial(\phi\rho_g)}{\partial t} + \frac{\partial(\phi\rho_g u)}{\partial x} = 0 \tag{1}$$

Species Mass Fraction Balance

$$\phi\rho_g \frac{\partial Y_k}{\partial t} + \phi\rho_g u \frac{\partial Y_k}{\partial x} + \frac{\partial(\phi\rho_g v_k Y_k)}{\partial x} - \phi\dot{\omega}_k MW_k = 0 \tag{2}$$

where v_k is the diffusion velocity and $\dot{\omega}_k$ the production rate of the k th species. Eqs. (1) and (2) assume the usual form of free-flame problems, however, with the IPM porosity (ϕ) multiplying all fluxes. The energy balances for the gas- and solid-phase are given as:

Gas-phase Energy Balance

$$\begin{aligned} & \phi\rho_g u C_{p,g} \frac{\partial T_g}{\partial x} - \frac{\partial}{\partial x}\left(\phi k_g \frac{\partial T_g}{\partial x}\right) - \phi \sum_k \rho_g C_{p,k} v_k \frac{\partial T_g}{\partial x} \\ + \quad & \phi \sum_k \dot{\omega}_k h_k + H_v(T_g - T_s) = 0 \end{aligned} \tag{3}$$

Solid-phase Energy Balance

$$- \quad \frac{\partial}{\partial x}\left(k_{eff} \frac{\partial T_s}{\partial x}\right) - H_v(T_g - T_s) + \frac{\partial Q_r}{\partial x} = 0 \tag{4}$$

Note that Eqs. (3) and (4) are coupled by the convective heat exchange term $H_v(T_g - T_s)$, in which the volumetric convective heat transfer coefficient (H_v) is described by the following correlation [20]:

$$Nu = 0.3 + 0.664 Pr^{1/3} Re^{1/2} \qquad Nu = \frac{H_v d_p}{k_g a_v} \qquad Re = \frac{\phi\rho_g u d_p}{\mu_g} \tag{5}$$

The IPM is assumed to be a 10 PPI SiC porous foam. The thermal conductivity of the SiC ceramic material (k_s) is given as function of the solid-phase temperature (T_s) [21]. The effective IPM conductivity (k_{eff}), appearing in Eq. (4), is obtained by the parallel arrangement model: $k_{eff} = (1-\phi)k_s$ (assuming $k_s >> k_g$) [22].

Regarding the thermal radiation modeling, the solid-phase is assumed to be a diffuse, grey body together with a non-participating gas-phase. The radiation heat transport term $\partial Q_r/\partial x$, in Eq. (4), is obtained from the solution of the one-dimensional radiative heat

transfer equations, which are numerically solved using the Discrete-Ordinates method (S_2 approximation) [23].

The species production rates ($\dot{\omega}_k$) of the methane TPOx process, required in Eqs. (2) and (3), are calculated using a $C1-C2$ detailed reaction mechanism (featuring 30 species and 154 elementary reactions) that is based on the model of Lindstedt et al. [24].

A schematic of the computational domain is shown in Figure 1, along with a representative temperature profile of a submerged flame. The IPM inlet and outlet surfaces coincide with the boundaries of the computational domain. These are extended upsteam and downstream far from the reaction front region in order to ensure that the submerged flames are 'blind' to the boundaries.

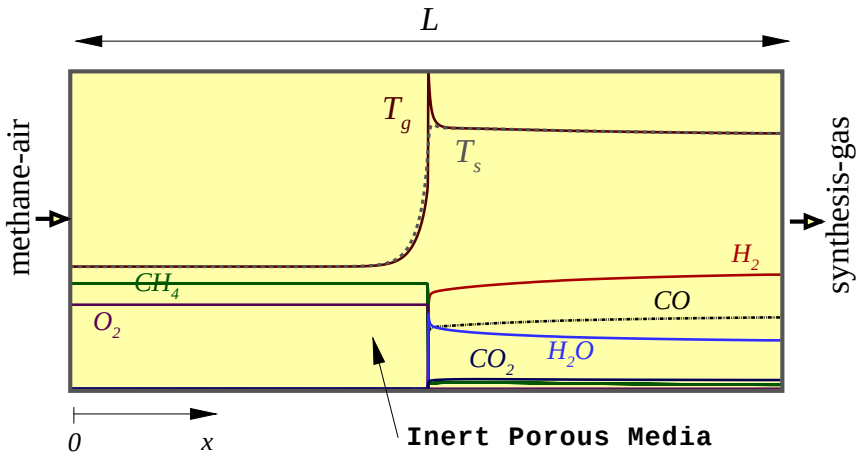

Figure 1: Representation of the computational domain ($L = 1$ m), including deterministic temperature and main species profiles for a submerged TPOx reaction with the following mixture conditions: $\lambda = 0.4$ and $T_{in} = 823$ K.

Regarding the boundary conditions (b.c.) imposed, the gas-phase species balance, Eq. (2), and the gas-phase energy balance, Eq. (3), are closed with Dirichlet and Neumann b.c. at the inlet and outlet of the computational domain, respectively. The b.c. for the mass balance, Eq. (1), is implicitly imposed by fixing the flame location. This is done by prescribing the gas-phase temperature at one point, see [19]. The inlet and outlet b.c. for the solid-phase energy balance, Eq. (4), are given by energy balances at the IPM surfaces:

Solid-phase Inlet b.c.

$$-\ k_s \frac{\partial T_s}{\partial x} - H_s(T_g - T_s) + \varepsilon\sigma(T_s^4 - T_{in}^4) = 0 \tag{6}$$

Solid-phase Outlet b.c.

$$k_s \frac{\partial T_s}{\partial x} - H_s(T_g - T_s) + \varepsilon\sigma(T_s^4 - T_{out}^4) = 0 \tag{7}$$

where $H_s = H_v/a_v$; T_{in} and T_{out} are assumed to be equal to the gas-phase temperature at the inlet and outlet of the computational domain, respectively. The b.c. for the radiative heat transfer equations are specified assuming that the inlet and outlet boundaries of the computational domain behave as black surfaces and are at a temperature equal to T_{in} and T_{out}, respectively.

2.2 Uncertain Parameters

For the present study, one consider the IPM to be the only source of parametric uncertainty. The influence of the IPM heat transfer phenomena on the combustion process model rely on correlations and coefficients that are assumed to possess some uncertainty level. The prescribed uncertain parameters are: the characteristic pore structure dimension (d_p); the IPM surface area per unit volume (a_v); the IPM porosity (ϕ); the solid conductivity (k_s); the radiative extinction coefficient (β); and the radiative scattering albedo (ω). The β and ω parameters directly influence the one-dimensional radiative heat

uncertain parameter	mean value	UF		Ref.
		limits	c_v	
d_p	6×10^{-4} m	1 ± 0.25	12.5 %	[25]
a_v	500 m^{-1}	1 ± 0.40	20 %	[25]
ϕ	0.88	1 ± 0.06	3 %	[25]
k_s	$f(T_s)$	1 ± 0.16	8 %	[21]
β	115 m^{-1}	1 ± 0.18	9 %	[8, 9]
ω	0.77	1 ± 0.18	9 %	[8, 9]

Table 1: Stochastic information of the uncertain parameters (where c_v is the coefficient of variation defined as [standard deviation]/[mean value]).

transfer equation system, on which the term $\partial Q_r/\partial x$, appearing in Eq. (4), depends.

All the uncertain parameters are assumed to have an half circle Beta distribution, in order to prevent unrealistic values that could occur with a Normal distribution. Each parameter distribution is parameterized by multiplying an uncertainty factor UF to the parameter mean value. This UF presents an half circle Beta PDF centered in 1, and the respective distribution limits are estimated based on realistic information obtained from producers or experimental sources. For some parameters, a safety coefficient of 2 is applied in the definition of these limits in order to tolerate possible lacks of probabilistic information. Table 1 resumes the stochastic information used for the uncertain parameters, as well as the references on which this information is based.

2.3 Uncertainty Quantification Procedure

This section describes the uncertainty quantification procedure used in the present work. As mentioned earlier, it is used a Non-Intrusive Spectral Projection (NISP) approach, where the deterministic model (described in section 2.1) is used in order to further post-process information about the propagation of uncertainty from the model input parameters into the model solution variables. This approach is preferred since it does not require a reformulation of the model governing equations, which is impractical for the present case due to the complexity of the model and the high number of uncertain parameters.

Let X be an uncertain parameter of the model, and f a corresponding solution variable. In general, for a prescribed PDF of X, one can represent $X(\xi)$ using a PC expansion given by Eq. (8) in terms of a random variable ξ;

$$X(\xi) = \sum_{j=0}^{p} c_n^X I_n(\xi) \tag{8}$$

with known expansion mode coefficients c_n^X, and where I_n, for $n = 0, .., p$, are orthogonal polynomials of order n. Depending upon the PDF of X there exists an optimal set of orthogonal polynomials I_n, with an associated random variable ξ, which minimizes the required number of terms in the PC expansion (8). If Normal or LogNormal PDFs are chosen for X then Hermite polynomials associated to a standard Normal random variable ξ are preferred; for Beta PDFs, Jacobi polynomials associated to a standard Beta random variable ξ should be used; a complete description of PC basis can be found in [12].

The problem can be further generalized for N independent uncertain parameters $(X_1, ..., X_N)$, with each one being associated with a stochastic dimension $\xi_i,\ i = 1, ..., N$, forming a multi-dimensional random space. In a general form, the multi-dimensional orthogonal polynomials are given as;

$$I_n(\vec{\xi}) = \begin{cases} I_0 & \\ I_1(\xi_i) & ,\ i = 1, ..., N \\ I_2(\xi_i, \xi_j) & ,\ i, j = 1, ..., N;\ \ j \leq i \\ I_3(\xi_i, \xi_j, \xi_k) & ,\ i, j, k = 1, ..., N;\ \ k \leq j \leq i \\ ... & \end{cases} \tag{9}$$

where $\vec{\xi} = (\xi_1, ..., \xi_N)$ is the vector of random variables. For each polynomial order n there exist a number, equal to $\max\{1; [\mathrm{N} \cdot ... \cdot (\mathrm{N} + \mathrm{n} - 1)]/\mathrm{n}!\}$, of distinct polynomials. These multi-dimensional polynomials can be generated from the uni-dimensional polynomials using tensor products. For notational convenience, the polynomials $I_n(\vec{\xi})$ are often renumbered in a convenient form in order to describe them with only one index, $\Phi_j(\vec{\xi})$, where there is a one-to-one correspondence between $I_n(\vec{\xi})$ and $\Phi_j(\vec{\xi})$ [12]. These polynomials are orthogonal to each other with respect to their inner product which takes the form;

$$< \Phi_i \Phi_j >= \int \Phi_i \Phi_j W(\vec{\xi}) d\vec{\xi} =< \Phi_j^2 > \delta_{ij} \tag{10}$$

where δ_{ij} is the Kronecker delta function; $W(\vec{\xi}) = w(\xi_1) \cdot ... \cdot w(\xi_N)$ is the weighting function of the corresponding PC basis $\{\Phi_j\}$, and $w(\xi_i), \ \forall i \in \{1, ..., N\}$ takes the same form of the PDF of ξ_i, see, *e.g.*, [12].

The stochastic solution variable $f(\vec{\xi})$ can also be represented in a similar manner as in Eq. (8), by using a multi-dimensional PC expansion, given as;

$$f(\vec{\xi}) = \sum_{j=0}^{P} c_j^f \Phi_j(\vec{\xi}) \tag{11}$$

where c_j^f are the unknown PC expansion mode coefficients of $f(\vec{\xi})$, and $P + 1 = (N + p)!/(N!p!)$ is the total number of terms in the PC expansion (with p being equal to the maximum polynomial order of the expansion).

Starting with Eq. (11) and applying the orthogonality relation in Eq. (10) on the complete basis $< \cdot \ \Phi_k >$, the coefficients c_j^f can be obtained as;

$$c_k^f = \frac{< f(\vec{\xi}) \Phi_k >}{< \Phi_k^2 >}, \ \ k = 0, ..., P \tag{12}$$

The final objective is to determine the coefficients c_k^f, which allow the reconstruction of the stochastic solution $f(\vec{\xi})$, using Eq. (11). This can be performed in a very effective manner using the ISP approach, *i.e.*, by solving the evolution of c_k^f. However, that implies the reformulation of the model governing equations, which is impractical for the present case. Therefore, the alternative NISP approach is preferred, where the deterministic solution f_d is evaluated for different values of $(X_1, ..., X_N)$. Further, by using Eq. (12), the coefficients c_k^f can then be calculated from these deterministic solutions and thereby the PC expansion of $f(\vec{\xi})$ can be easily reconstructed from Eq. (11).

The overall NISP approach used here involves the following procedure:

1. According to the prescribed PDF for the parameters $X_i, \ \ i = 1, ..., N$, the respective random variables $\xi_i, \ \ i = 1, ..., N$ assume a distribution type associated to a particular PC basis $\{\Phi_j\}$. The vector of random variables, $\vec{\xi} = (\xi_1, ..., \xi_N)$ is sampled on $\{\vec{\xi^n}\}_{n=1}^S$ selected collocation points, as explained further.

2. For each sample $\vec{\xi^n}$, the corresponding sample vector of input parameters, $(X_1^n, ..., X_N^n)$ is calculated from Eq. (8), or alternatively, from a know function $X_i = g(\xi_i)$.

3. The solution of the deterministic model f_d^n is computed for all the realizations of the input parameters vector, $\{(X_1^n, ..., X_N^n)\}_{n=1}^S$.

4. The PC expansion mode coefficients c_k^f are then obtained by numerically solving Eq. (12). The integral in the numerator of Eq. (12) is here approximated by a Gauss quadrature [13, 14]. This implies that each random variable $\xi_i, \ \forall i \in \{1, ..., N\}$, in the vector $\vec{\xi}$, must be sampled on S_i different collocation points (Gauss quadrature points), which are the roots of the unidimensional orthogonal polynomial $I_r(\xi_i)$ of order $r = S_i$. The required number of multidimensional samples $S = \prod_{i=1}^{N} S_i$ depends upon the smoothness of the stochastic solution $f(\vec{\xi})$. By applying the Gauss quadrature in order to compute the integral in the numerator of Eq. (12), the mode coefficients of the stochastic solution PC expansion are numerically approximated as;

$$c_k^f \approx \frac{\sum_{r_1,...,r_N=1}^{S_1,...,S_N} f_d(X_{r_1}, ..., X_{r_N}) \Phi_k(\xi_{r_1}, ..., \xi_{r_N}) \prod_{i=1}^{N} q_{r_i}}{< \Phi_k^2 >}, \ \ k = 0, ..., P \tag{13}$$

where $(\xi_{r_i}, q_{r_i}), \ r = 1, ..., S_i$, are the Gauss quadrature points and corresponding weights, sampled on the random variable $\xi_i, \ \forall i \in \{1, ..., N\}$.

The post-processing of information about the stochastic solutions is performed using the PC expansion mode coefficients calculated previously. The solution statistics (mean and standard deviation) are easily obtained by applying the properties of orthogonal polynomials to the definition of each statistics. The solutions PDFs are approximated by employing Kernel Density Estimation techniques [26], and the CIs are further calculated from the respective Cumulative Density Functions (CDFs).

3 NUMERICAL RESULTS

The parametric uncertainty quantification results for the model of methane-air TPOx within IPM are presented in this section. Propagation of parametric uncertainty through the model is quantified prescribing uncertainty in six parameters ($N = 6$) related with the IPM heat transfer phenomena, see Table 1. The uncertainty quantification is first investigated for a particular set of methane-air TPOx conditions: air-fuel ratio (λ) of 0.4 and inlet mixture temperature (T_{in}) of 823 K. Further, the stochastic solution variables are calculated for different values of λ and T_{in} in order to investigate their influence on the uncertainty propagation.

3.1 Uncertainty in the IPM heat transfer parameters

The PC expansion coefficients of the stochastic solution variables are obtained applying the NISP approach described in section 2.3. The stochastic solution variables are approximated by second-order PC expansions, which was found to be sufficient for accuracy in the present case. The deterministic solution space is sampled using $S_i = 3$ collocation

points in each uncertain parameter, therefore, requiring $3^6 = 729$ runs with the deterministic model. The computational time required for the total calculation was ~ 300 min in a P4 1.7 GHz/ 1024 MB (~ 240 min for the deterministic solution samples and ~ 20 min for the stochastic information post-processing).

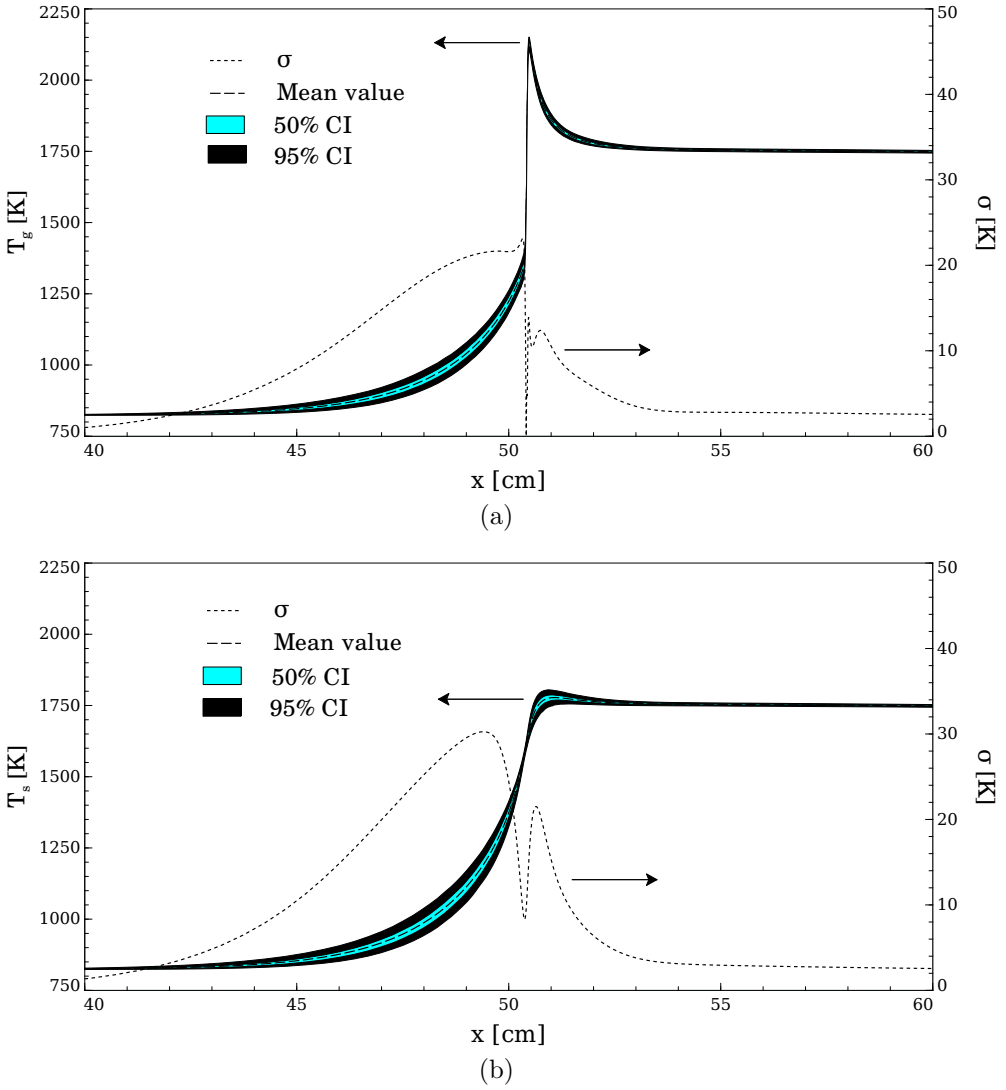

Figure 2: Stochastic mean solution profiles, along with the 50 % and 95 % CIs and standard deviation (σ) for the methane-air TPOx ($\lambda = 0.4$; $T_{in} = 823$ K): (a) gas-phase temperature; (b) solid-phase temperature.

Figures 2(a) and (b) show the stochastic mean solution profiles for the gas-phase temperature (T_g) and solid-phase temperature (T_s), respectively, along with the 50 % and

95 % CIs and standard deviation (σ). One can observe from the figures that the uncertainty level of both T_g and T_s is maximum at the flame front region, where the heat recirculation takes place. Far upstream and downstream from the flame front region, the uncertainty level falls close to zero since there is negligible heat transfer taking place. However, in the downstream region there is some remaining uncertainty that decreases slowly and it can be explained by the ongoing slow reforming reactions, which affect the downstream heat release. Furthermore, one may also note that the uncertainty level of T_s is slightly higher than the one of T_g, which is in agreement with the model set-up since the uncertainty sources are directly related with the solid-phase heat transfer.

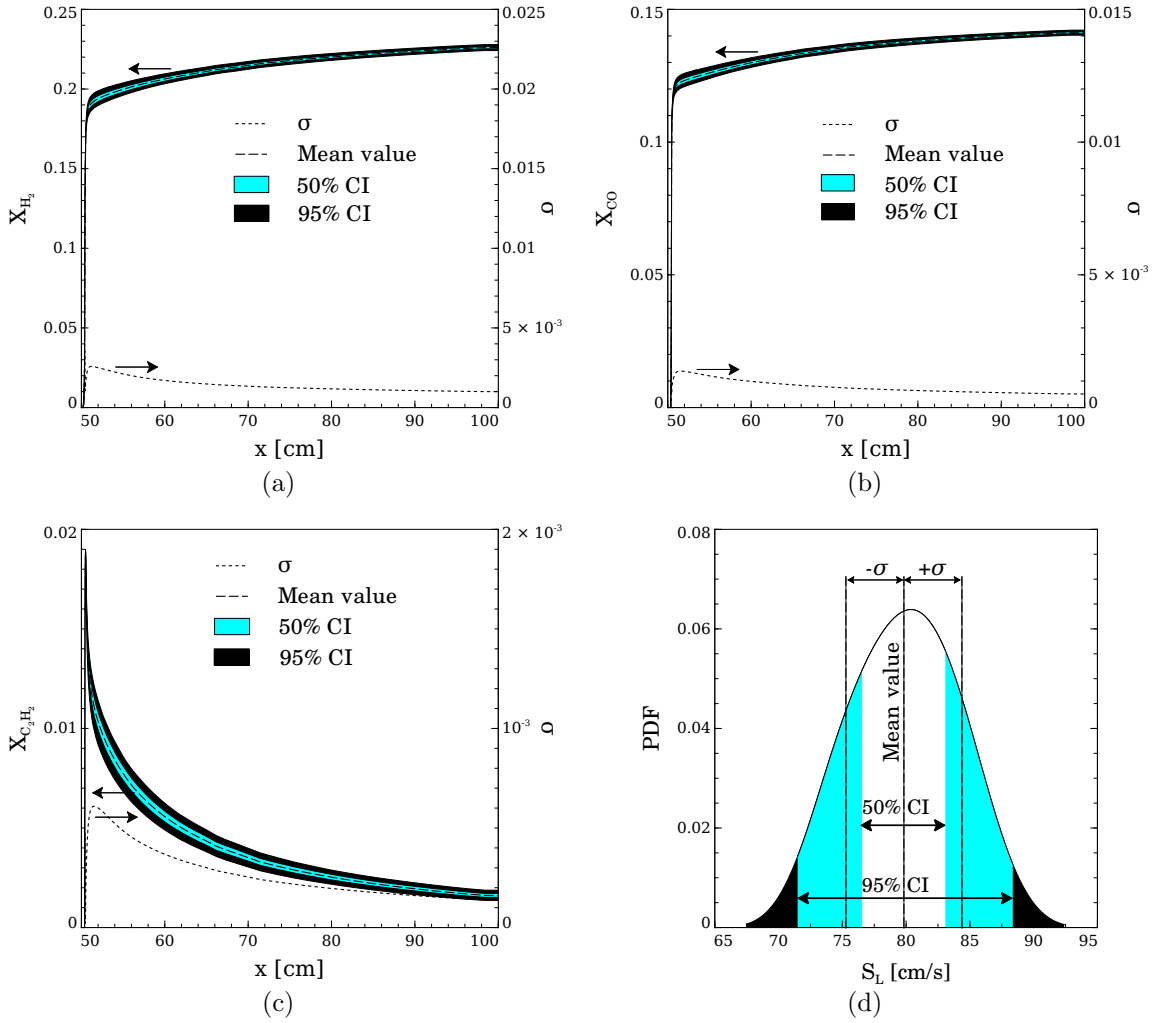

Figure 3: Stochastic mean solution profiles, along with the 50 % and 95 % CIs and standard deviation (σ) for the methane-air TPOx ($\lambda = 0.4$; $T_{in} = 823$ K): (a) H_2 molar fraction; (b) CO molar fraction; (c) C_2H_2 molar fraction; (d) laminar burning velocity PDF.

Figures 3(a), (b), (c) present the stochastic mean solution profiles for the H_2, CO and $C2H2$ molar fractions, respectively, along with the 50 % and 95 % CIs and standard deviation. One can observe from these figures that the uncertainty level of X_{H_2}, X_{CO} and $X_{C_2H_2}$ decreases along the post-flame region, however, in a very slow manner due to the ongoing reforming reactions referred above. Furthermore, the quantitative comparison of the standard deviation with the respective mean value, reveals that the relative uncertainty level of X_{H_2}, X_{CO} is lower than the one of $X_{C_2H_2}$.

The PDF of the laminar burning velocity (S_L) is shown in Figure 3(d), along with the 50 % and 95 % CIs, mean value and standard deviation. One can observe from the figure that the PDF presents a small asymmetry as well as positive and negative tails, in opposition to the half circle Beta PDF prescribed to the uncertain parameters. This can be explained by the non-linearities in the governing equations that affect the uncertainty propagation through the physical model.

Figures 4(a), (b), (c), (d), (e) and (f) present the PC expansion coefficients that represent the first-order contribution of the uncertain parameters to the total uncertainty in the stochastic solutions for T_g, T_s, X_{H_2}, X_{CO}, $X_{C_2H_2}$ and S_L, respectively. One can identify from these figures which are the dominant uncertain parameters. One may note that the relative contribution of each parameter to the total uncertainty is not the same for all the solution variables and depends on the axial coordinate (x). However, the contribution of each parameters, ordered from the strongest to the weakest, is generally the following: a_v, ϕ, d_p, k_s, ω and β. The strong influence of a_v can be attributed to the high level of uncertainty prescribed to it, see Table 1. Regarding the ϕ parameter, its strong influence is rather explained by the way it deeply affects the model governing equations, although it presents a low level of uncertainty, see Table 1.

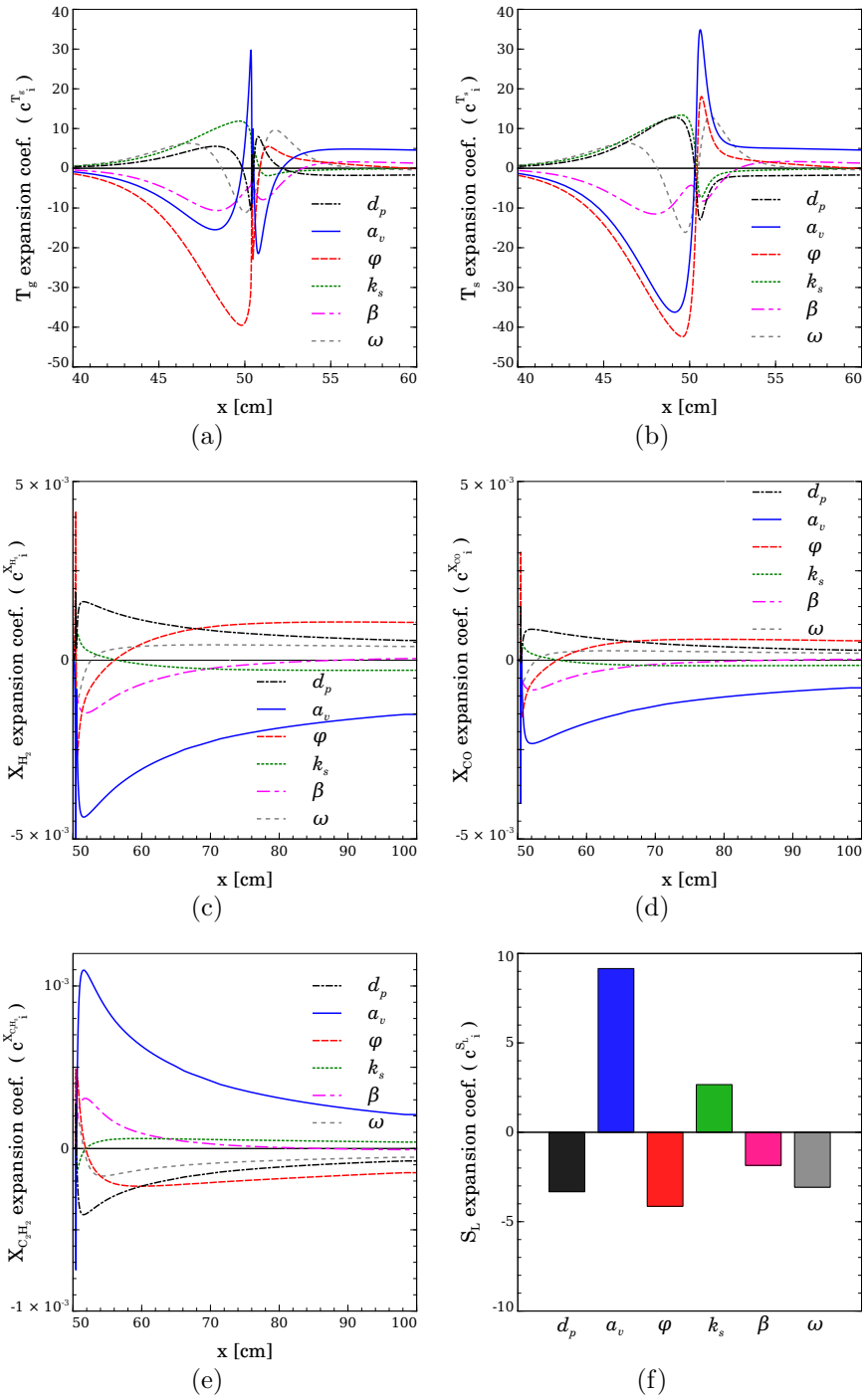

Figure 4: Spectral decomposition of the stochastic solution, showing the PC expansion coefficients that represent the first-order contribution of the each uncertain parameter to the total uncertainty for the methane-air TPOx ($\lambda = 0.4$; $T_{in} = 823$ K): (a) gas-phase temperature; (b) solid-phase temperature; (c) H_2 molar fraction; (d) CO molar fraction; (e) C_2H_2 molar fraction; (f) laminar burning velocity.

3.2 Influence of inlet mixture conditions on uncertainty propagation

In the following, one investigates the effect of the air-fuel ratio, λ, and the inlet mixture temperature, T_{in}, on the relative uncertainty level of the stochastic solution variables. Simulations are carried out for λs is the range of $0.38 - 0.42$ and T_{in} in the range of $723 - 923$ K, and the relative uncertainty level is quantified by the coefficient of variation ($c_v = \sigma/Mean$).

The numerical results reveal that the influence of λ on the relative uncertainty level of T_g, T_s and S_L is negligible. The maximum c_v value for T_g and T_s is in the range of $1.98 \pm 0.04\%$ and $2.68 \pm 0.07\%$, respectively, and for S_L, the c_v value is in the range of $5.68 \pm 0.06\%$. Although the influence of T_{in} on T_g, T_s and S_L is slightly stronger that the influence of λ, it continues to be negligible. The maximum c_v value for T_g and T_s is in the range of $2.10 \pm 0.48\%$ and $2.75 \pm 0.41\%$, respectively, and the c_v value for S_L is in the range of $5.66 \pm 0.13\%$. Furthermore, the c_v value increases (negligibly) with λ for all the three stochastic variables (T_g, T_s and S_L) and a similar evolution of c_v is found with respect to T_{in}.

Figures 5(a), (c) and (e) show the effect of λ on the c_v profile for X_{H_2}, X_{CO} and $X_{C_2H_2}$, respectively. The c_v of $X_{C_2H_2}$ assumes values approximately one order of magnitude higher than the c_v values of X_{H_2} and X_{CO}. Furthermore, the c_v of $X_{C_2H_2}$ increases with λ, however, the opposite is found for X_{H_2} and X_{CO}.

Figures 5(b), (d) and (f) show the effect of T_{in} on the c_v profile for X_{H_2}, X_{CO} and $X_{C_2H_2}$, respectively. In a similar way to what was found for λ, the c_v values of $X_{C_2H_2}$ are approximately one order of magnitude higher than the ones of X_{H_2} and X_{CO}. The c_v of $X_{C_2H_2}$ also increases with T_{in} and the opposite happens for X_{H_2} and X_{CO}.

Although the influence of λ and T_{in} on the c_v profiles for the X_{H_2} and X_{CO} is non negligible, the low values assumed by c_v for both X_{H_2} and X_{CO} make this finding less relevant. However regarding $X_{C_2H_2}$, the high level of relative uncertainty denoted by the c_v profile makes the influence of λ and T_{in} to be importante on the uncertainty quantification for $X_{C_2H_2}$.

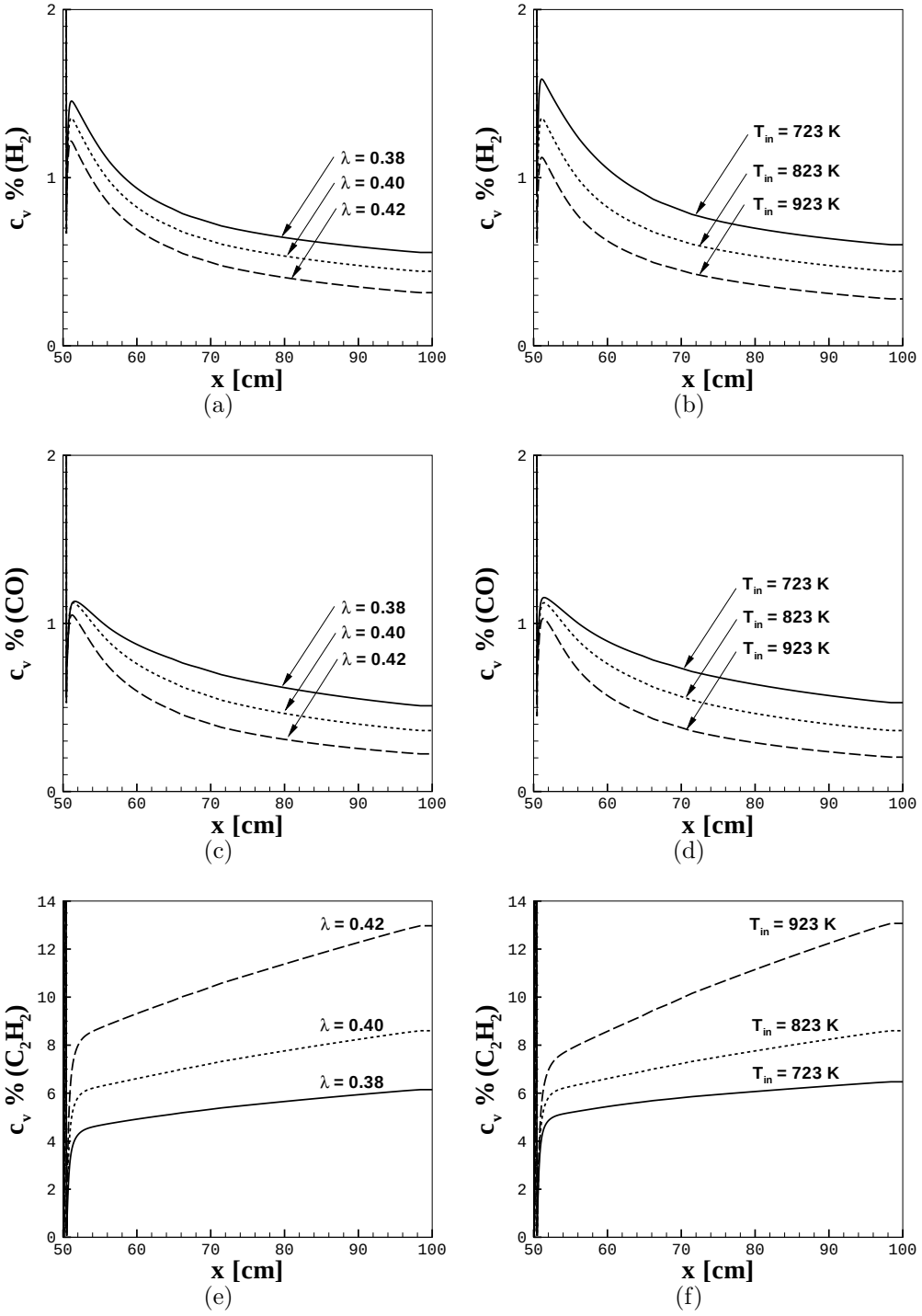

Figure 5: Effect of the inlet mixture conditions on the coefficient of variation for the methane TPOx. Effect of the air-fuel ratio λ fixing $T_{in} = 823$ K: (a) H_2 molar fraction; (c) CO molar fraction; (e) C_2H_2 molar fraction. Effect of the inlet mixture temperature T_{in} fixing $\lambda = 0.40$: (b) H_2 molar fraction; (d) CO molar fraction; (f) C_2H_2 molar fraction.

4 CONCLUSIONS

The propagation of parametric uncertainty through a physical model is investigated for the problem of methane-air TPOx within IPM. The combustion model includes a detailed $C1-C2$ reaction mechanism and solves the gas- and solid-phase energy balances coupled by convective heat exchange, including radiative heat transfer in the solid-phase. The parametric uncertainty quantification is carried out by applying a Non-Intrusive Spectral Projection based method, which uses the deterministic physical model as a black box. Uncertainty is prescribed in six model parameters related with the IPM heat transfer phenomena. These uncertain parameters are modeled as an half circle Beta distribution and their probabilistic information is prescribed based on producers or experimental sources. The PC expansion mode coefficients of the stochastic solution variables are obtained using a set of deterministic solutions, which are previously calculated sampling the uncertain parameters on the Gauss-Jacobi quadrature points of the Beta distributions. Statistics, CIs and PDFs are post-processed from the PC expansion coefficients for the gas- and solid-phase temperatures, H_2, CO and C_2H_2 molar fractions and laminar burning velocity. The uncertainty quantification analysis is first carried out for a particular set of methane-air TPOx conditions: air-fuel ratio of 0.4 and inlet mixture temperature of 823 K. Further, it is investigated the effect of the air-fuel ratio and inlet mixture temperature on the stochastic solution variables.

The main conclusions can be drawn from the present study:

1. Gas- and solid-phase temperature predictions presented a higher uncertainty level at the flame front region, and the uncertainty level for the solid-phase temperature was slightly higher than the one for the gas-phase temperature.

2. The uncertainty level in predicting the H_2, CO and $C2H2$ molar fractions varies smoothly along the post-flame region. Moreover, the relative uncertainty level for $C2H2$, given by c_v, is one order of magnitude higher than the one for H_2 and CO.

3. The comparison of the first-order PC expansion coefficients show that, in general, the IPM specific surface area and the IPM porosity are the main responsible for the uncertainty in the stochastic solution variables, and in opposition, the parameters directly related with the radiative heat transfer (extinction coefficient and scattering albedo) present the weakest contribution.

Regarding the effect of the air-fuel ratio, λ, and inlet mixture temperature, T_{in}, on the the stochastic solution variables, the additional conclusions are found:

4. The influence of the air-fuel ratio and inlet mixture temperature on c_v is negligible for the gas- and solid-phase temperatures and the laminar burning velocity; however, not for the H_2, CO and $C2H2$ species molar fractions.

5. The c_v increases with the air-fuel ratio and inlet mixture temperature for the $C2H2$ species and the opposite was found for the H_2 and CO species.

ACKNOWLEDGEMENTS

The first author would like to acknowledge the financial support through scholarship from Fundação para a Ciência e a Tecnologia - FCT.

REFERENCES

[1] J.D. Holladay, J. Hu, D.L. King, Y. Wang, An overview of hydrogen production technologies, *Catalysis Today*, **139**, 244–260 (2009).

[2] Z. Al-Hamamre, S. Voss, D. Trimis, Hydrogen production by thermal partial oxidation of hydrocarbon fuels in porous media based reformer, *International Journal of Hydrogen Energy*, **34**, 827-832 (2009).

[3] J.R. Howell, M.J. Hall, J.L. Ellzey, Combustion of hydrocarbon fuels within porous inert media, *Progress in Energy and Combustion Science*, **22**, 121–145 (1996).

[4] M. Abdul Mujeebu , M.Z. Abdullah, M.Z. Abu Bakar, A.A. Mohamad, R.M.N. Muhad, M.K. Abdullah, Combustion in porous media and its applications - A review, *Journal of Environmental Management*, **86**, 1365–1375 (2009).

[5] A.J. Barra, J.L. Ellzey, Heat recirculation and heat transfer in porous burners, *Combustion and Flame*, **137**, 230–241 (2004).

[6] X.Y. Zhou, J.C.F. Pereira, Numerical study of combustion and pollutants formation in inert nonhomogeneous porous media, *Combustion Science and Technology*, **130**, 335–364 (1997).

[7] R.S. Dhamrat, J.L. Ellzey, Numerical and experimental study of the conversion of methane to hydrogen in a porous media reactor, *Combustion and Flame*, *144*, 698–709 (2006).

[8] X. Fu, R. Viskanta, J.P. Gore, A model for the volumetric radiation characteristics of cellular ceramics, *International Communications in Heat and Mass Transfer*, **24**, 1069–1082 (1997).

[9] K. Pickenäcker, Emissionsarme kompakte Gasheizsysteme auf der Basis stabilisierter Verbrennung in porösen Medien, VDI-Verlag, PhD Dissertation, University of Erlangen, Germany (2001).

[10] K. Kamiuto, S.S. Yee, Heat transfer correlations for open-cellular porous materials, *International Communications in Heat and Mass Transfer*, **32**, 947–953 (2005).

[11] P. Colombo, Ceramic foams: fabrication, properties and applications, *Key Engineering Materials*, **206-213**, 1913–1918 (2002).

[12] D. Xiu, G.E. Karniadakis, Modeling uncertainty in flow simulations via generalized polynomial chaos, *Journal of Computational Physics*, **187**, 137–167 (2003).

[13] O.M. Knio, O.P. LeMaître, Uncertainty propagation in CFD using polynomial chaos decomposition, *Fluid Dynamics Research*, **38**, 616–640 (2006).

[14] H.N. Najm, Uncertainty quantification and polynomial chaos techniques in computational fluid dynamics, *Annual Review of Fluid Mechanics*, **41**, 35–52 (2009).

[15] M.A. Tatang, Direct incorporation of uncertainty in chemical and environmental engineering systems, PhD thesis, MIT (1995).

[16] D.G. Cacuci, Sensitivity and Uncertainty Analysis: Theory, Volume I, *Boca Raton: Chapman & Hall/CRC* (2003).

[17] O.P. Le Maître, O.M. Knio, H.N. Najm, R.G. Ghanem, A stochastic projection method for fluid flow: I. Basic formulation, *Journal of Computational Physics*, **173**, 481–511 (2001).

[18] B. Ganapathysubramanian, N. Zabaras, Sparse grid collocation schemes for stochastic natural convection problems, *Journal of Computational Physics*, **225**, 652–685 (2007).

[19] R.J. Kee, J.F. Grcar, M.D. Smooke, J.A. Miller, A Fortran program for modelling steady laminar one-dimensional premixed flames, *Report SAND85- 8240, Sandia National Laboratories* (1996).

[20] M. Scheffler, P. Colombo (Eds.), Cellular ceramics: Structure, manufacturing, properties and applications, *Weinheim: Wiley VCH Verlag* (2005).

[21] R.G. Munro, Material Properties of a Sintered alpha-SiC, *Journal of Physical and Chemical Reference Data*, **26**, 1195–1203 (1997).

[22] M. Kaviany, Principles of Heat Transfer in Porous Media, *New York: Springer-Verlag*, pag. 126 (1991).

[23] M.F. Modest, Radiative Heat Transfer, *New York: McGraw-Hill*, pag. 546 (1993).

[24] P. Lindstedt, L. Maurice, M. Meyer, Thermodynamic and kinetic issues in the formation and oxidation of aromatic species, *Faraday Discussions*, **119**, 409–432 (2001).

[25] A. Mach, Entwicklung eines kompakten Heizsystems für Heizöl EL auf Basis der Verbrennung in porösen Keramiken, PhD Dissertation, University of Erlangen, Germany (2007).

[26] A.J. Izenman, Recent Developments in Nonparametric Density Estimation, *Journal of the American Statistical Association*, **86**, 205–224 (1991).